5-2021

The diversity and evolution of phenazine biosynthesis pathways in Enterobacterales

Christian Leise

The diversity and evolution of phenazine biosynthesis pathways in Enterobacterales

by

Christian Leise

A Thesis
Submitted to the Honors College of
The University of Southern Mississippi
in Partial Fulfillment
of Honors Requirements

May 2021

Approved by:

Dmitri Mavrodi, Ph.D., Thesis Advisor,
School of Biological, Environmental and Earth Sciences

Jake Schaefer, Ph.D., Director,
School of Biological, Environmental and Earth Sciences

Ellen Weinauer, Ph.D., Dean
Honors College

ABSTRACT

Enterobacterales is an order of Gram-negative bacteria that encompasses plant and animal pathogens and organisms of industrial importance. Some of these bacteria produce secondary metabolites classified as phenazines (Phz). Studies in other groups of microorganisms revealed that phenazines are redox-active and exhibit broad antibacterial, antifungal, and antiparasitic activity. *Enterobacterales* are known to produce phenazines, but details about the diversity, biochemistry, and function of phenazine metabolites in these organisms are missing. In this work, we screened the National Center for Biotechnology Information (NCBI) GenBank for genome sequences of phenazine-producing (Phz+) *Enterobacterales*. Additionally, genomes of Phz+ strains *Pectobacterium carotovorum* cc303 and *P. betavasculorum* Ecb168 were sequenced, assembled, annotated, and used in downstream analyses. Scaffolds containing *phz* clusters were extracted and analyzed for the presence of the core biosynthesis, phenazine modifying, and resistance genes. These deoxyribonucleic acid (DNA) sequences were analyzed for the presence of site-specific recombinases and transposases. The evolution of *phz* pathways was analyzed by comparing phylogenies of the core phenazine biosynthesis and housekeeping genes. The results of this study revealed an unexpected and widespread presence of phenazine genes in *Enterobacterales.* We identified at least six distinct types of phenazine clusters in *Escherichia coli, Shigella, Klebsiella, Enterobacter, Pantoeae, Brenneria, Serratia, Xenorhabdus*, *Photorhabdus*, and *Providencia*. In many strains, *phz* genes formed parts of genomic islands or were associated with plasmids, suggesting their spread via horizontal gene transfer and contribution to the competition for the ecological niche between closely related taxa.

Keywords: *Enterobacterales*, phenazine, biosynthesis, evolution, horizontal gene transfer, mobile genetic elements

DEDICATION

To my loving wife, who has been with me every step of the way, to all of my friends, who have celebrated my triumphs and aided me in times of stress, and especially to my family, who have always supported and believed in me.

ACKNOWLEDGMENTS

My sincere gratitude to Dr. Dmitri Mavrodi for his guidance throughout this research cannot be overstated. He was incredibly patient and insightful in his teaching, and without his knowledge and advice this thesis would not have been possible. Furthermore, I would like to thank The University of Southern Mississippi (USM) and the USM Honors College for providing me the opportunity to conduct undergraduate research and produce a thesis; it has been invaluable to my undergraduate experience. Finally, I would like to thank the funding source of my research, the Drapeau Center for Undergraduate Research.

TABLE OF CONTENTS

LIST OF TABLES

LIST OF ILLUSTRATIONS

LIST OF ABBREVIATIONS

ADIC	2-amino-2-deoxyisochorismic acid
AGA	D-alanylgriseoluteic acid
BLAST	basic local alignment search tool
CDS	coding sequence
CRISPR	clustered regularly interspaced short palindromic repeat
DHHA	trans-2,3-dihydro-3-hydroxyanthranilic acid
DOE	The United States Department of Energy
DNA	deoxyribonucleic acid
EC	Enzyme Commission
G+C	guanine + cytosine
GE	genomic island
GO	gene ontology
HGT	horizontal gene transfer
HHR	high ratio of hypothetical proteins
HMM	hidden Markov model
ICE	integrative and conjugative element
MAFFT	multiple alignment using fast fourier transform
MGE	mobile genetic element
MUSCLE	multiple sequence comparison by log-expectation
NCBI	National Center for Biotechnology Information
NJ	neighbor-joining
PATRIC	Pathosystems Resource Integration Center

PCA	phenazine-1-carboxylic acid
PDC	phenazine-1,6-dicarboxylic acid
Phz	phenazine
PYO	pyocyanin
PCN	phenazine-1-carboxamide
RNA	ribonucleic acid
USM	The University of Southern Mississippi

CHAPTER I: INTRODUCTION

Enteric bacteria are facultatively aerobic, Gram-negative, nonsporulating microorganisms within the *Gammaproteobacteria* (Octavia & Lang, 2014). Because of their medical importance, many genera and species of enteric bacteria have been characterized for identification in clinical microbiology. The most important pathogenic members include enterotoxigenic strains of *Escherichia coli*, *Salmonella*, and *Shigella*, which cause gastroenteritis in humans and animals. Closely related opportunistic pathogens *Klebsiella, Proteus*, *Enterobacter, Serratia*, and *Citrobacter* cause life-threatening urinary and respiratory tract infections. Many members of this group are capable of infecting both immunocompromised and healthy individuals and are becoming resistant to antibiotics (Boucher et al., 2009). The group also includes several plant pathogens, as well as species of industrial importance.

Some species of enteric bacteria produce phenazines (Phz). Naturally occurring phenazines are redox-active heterocyclic secondary metabolites that are synthesized via the shikimic acid pathway (Mavrodi et al., 2006). Most of them are broadly inhibitory to bacteria, fungi, and parasites, and some have antitumor activity. Numerous studies demonstrated that the inhibitory role of phenazines contributes to the competitiveness of their producers. Phenazines synthesized by symbiotic species of *Pseudomonas* in the plant rhizosphere suppress soilborne diseases caused by fungal pathogens (Thomashow & Weller, 1988). Pyocyanin, a phenazine synthesized by the human pathogen *Pseudomonas aeruginosa*, acts as a potent virulence factor during lung infections (Lau et al., 2004).

Despite recent progress in identifying phenazine pathways and diversity in *Pseudomonas*, a similar depth of knowledge on the diversity, biochemistry, and

biological functions of phenazines in other bacterial groups is missing. Preliminary studies in the Mavrodi lab revealed the presence of phenazine pathways in genomes of enteric bacteria, including some *E. coli* and *Klebsiella* spp. However, detailed information about phenazine pathways in this economically important group of microorganisms remains unexplored. My project aimed to address this significant gap in the knowledge by focusing on the diversity, organization, and evolution of phenazine pathways in species of *Enterobacterales*. I hypothesized that the patchy distribution of phenazine genes reflects their spread among enteric bacteria via horizontal gene transfer and contribution to the competition for the ecological niche between closely related taxa.

CHAPTER II: LITERATURE REVIEW

Taxonomy and importance of the order Enterobacterales

The *Enterobacterales,* commonly called the enteric bacteria, is one of the most significant orders within the *Gammaproteobacteria*. The order encompasses gram-negative, facultatively aerobic, nonsporulating bacteria, most of which are oxidase-negative, catalase-positive, and either nonmotile or motile by peritrichous flagella (Octavia & Lang, 2014). Members of this group also reduce nitrate to nitrite and produce acid during glucose fermentation, although these traits are not uniformly distributed across all taxa. Because of the medical importance, many enteric bacteria have been characterized, and numerous genera and species have been defined, mainly for ease in identification purposes in clinical microbiology. However, because enteric bacteria are genetically very closely related, their positive identification remains difficult (Ferone et al., 2020). Identification typically requires the analysis of a combination of diagnostic testing via miniaturized rapid diagnostic kits, DNA-based comparisons, and immunological assays.

The *Enterobacterales* are well studied genetically with 12,407 complete and draft genomes listed in the Department of Energy (DOE) Joint Genome Institute database (Chen et al., 2019) as of January 2021. The finished genomes range in size from 298,471 to 8,461,711 bp (mean 4,832,906 bp), coding between 297 and 8,189 genes (mean 4,780 genes). The Guanine + Cytosine (G+C) content varies between 17.8 and 60.1% with a mean value of 51.4%. The smallest genome belongs to the mealybug endosymbiont *Trabutina mannipara* TRABT (Szabo et al., 2017), while the species with the largest genome is the emerging foodborne pathogen *Cronobacter sakazakii*, which causes life-

threatening infections in newborns and infants (Blackwood & Hunter, 2016). The advent of genome sequencing triggered significant changes in the taxonomic classification of enteric bacteria, which were traditionally placed into one family, the *Enterobacteriaceae*. In 2016, Adeolu *et al*. (2016) conducted a comprehensive phylogenomic analysis of the group and proposed to combine all enteric bacteria into a new order, *Enterobacterales*, which is further divided into several families, including *Enterobacteriaceae*, *Pectobacteriaceae*, and other closely-related members. *Enterobacter* was proposed as the type genus of the order *Enterobacterales*.

Several species of enteric bacteria are pathogenic to humans, other animals, or plants, and among non-pathogenic species are other members of industrial relevance. *Escherichia coli*, the best studied prokaryote, is the classic enteric bacterium. It is commonly found as a member of the commensal gut microbiome in humans and other animals and can cause disease in nearly every tissue in the body (Octavia & Lang, 2014). *Klebsiella* spp. occupy a wider selection of ecological niches, and are associated with water, soil and plants, and humans and other animals. *Klebsiella pneumoniae* is especially significant as a contributor to drug-resistant nosocomial infections in neonatal intensive care units (Luo et al., 2020). *Xenorhabdus* spp. exist exclusively as gut endosymbionts of entomopathogenic nematodes and have not been found outside of their hosts in either soil or water (Octavia & Lang, 2014). *Pectobacterium* spp., including *P. atrosepticum*, *P. carotovorum*, and *P. betavasculorum* are phytopathogens known to cause a variety of diseases such as soft rot and wilt. Significantly, several *Pectobacterium* spp. cause blackleg in the stems of potato crops (van der Wolf et al., 2017). The isolation of most *Enterobacterales* is generally simple, as they grow readily in blood or chocolate

agar without specific atmospheric requirement and an *Enterobacteriaceae* enrichment broth has been developed to isolate *Enterobacterales* from food and environmental samples (Octavia & Lang, 2014).

The diversity and biosynthesis of phenazine metabolites

My project is focused on strains of *Enterobacterales* that produce biologically active secondary metabolites called phenazines. Naturally occurring phenazines include dozens of nitrogen-containing, heterocyclic, colored compounds (Laursen & Nielsen, 2004). Phenazines generally are water-soluble and often produced by bacteria in copious amounts (up to grams per liter) (Turner & Messenger, 1986). Most phenazines are redox-active and exhibit broad-spectrum antibiotic, antiparasitic, and/or antitumor activity due to their ability to interfere with the function of the respiratory chain and trigger the accumulation of reactive oxygen species (Hassan & Fridovich, 1980; Liu & Nizet, 2009).

The range of organisms capable of producing phenazines has been documented since the late 1960s (Turner & Messenger, 1986). All known phenazine producers belong to *Eubacteria*, except for the archaeon *Methanosarcina* that uses a membrane-embedded methanophenazine as an electron carrier during methanogenesis (Duszenko & Buan, 2017). Phenazine production is common among the high G+C Gram-positive bacteria, especially among different groups of *Actinobacteria* (Dar et al., 2020). Many of these are members of the genus *Streptomyces* that produce an impressive array of phenazine aldehydes, thioesters, esters, amides, and larger molecules that include side chains and carbohydrates as part of their structure (Laursen & Nielsen, 2004) (Figure 1). The Gram-negative *Proteobacteria* contain two clades of organisms that produce simpler products,

including hydroxyl-, carboxyl-, methoxy-, and methylester-substituted phenazine compounds.

Fluorescent pseudomonads include numerous well-documented producers, most of which belong to *P. fluorescens* and *P. aeruginosa* species complexes (Biessy et al., 2019). Species of the *P. fluorescens* complex produce only phenazine-1-carboxylic acid (PCA), while all other pseudomonads are able to synthesize two or more different derivatives. *Pseudomonas chlororaphis* sbsp. *aureofaciens* produces PCA, 2-hydroxy-PCA, and 2-hydroxyphenazine, while *P. chlororaphis* sbsp. *chlororaphis* produces phenazine-1-carboxylic acid and phenazine-1-carboxamide (Mavrodi et al., 2006). *Pseudomonas aeruginosa* is the first microorganism described as a phenazine producer, and its characteristic pigment pyocyanin (PYO) was described over 160 years ago (Vilaplana & Marco, 2020). PYO is synthesized by almost all *P. aeruginosa* isolates, which also may produce PCA, 1-hydroxyphenazine, phenazine-1-carboxamide, and aeruginosins A and B (Laursen & Nielsen, 2004; Mavrodi et al., 2001).

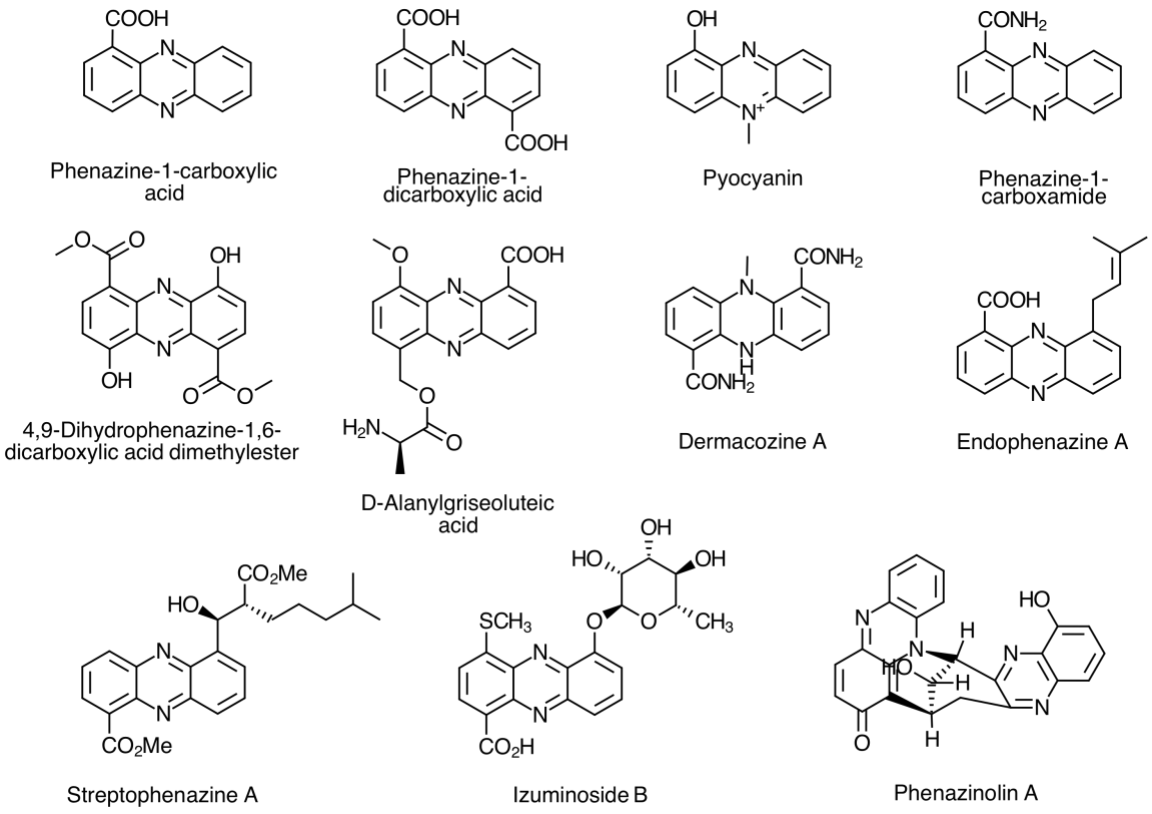

Figure 1. Structures of some naturally occurring microbial phenazines.

Other well-characterized phenazine-producing gamma *Proteobacteria* include *Pantoea agglomerans* Eh1087, which synthesizes D-alanylgriseoluteic acid (AGA) (Giddens et al., 2002), and *Lysobacter antibioticus* that produces the cherry-red antibiotic myxin (Turner & Messenger, 1986). Among beta *Proteobacteria*, phenazine production was reported in *Burkholderia cepacia* and *Paraburkholderia phenazinium* that produce multiple complex phenazine compounds (Korth et al., 1978; Turner & Messenger, 1986).

Phenazines are synthesized via the shikimic acid pathway, and their heterocyclic tricycle is formed through the head-to-tail condensation of two precursor molecules derived from chorismic acid (Guttenberger et al., 2017) (Figure 2). The nitrogen for this

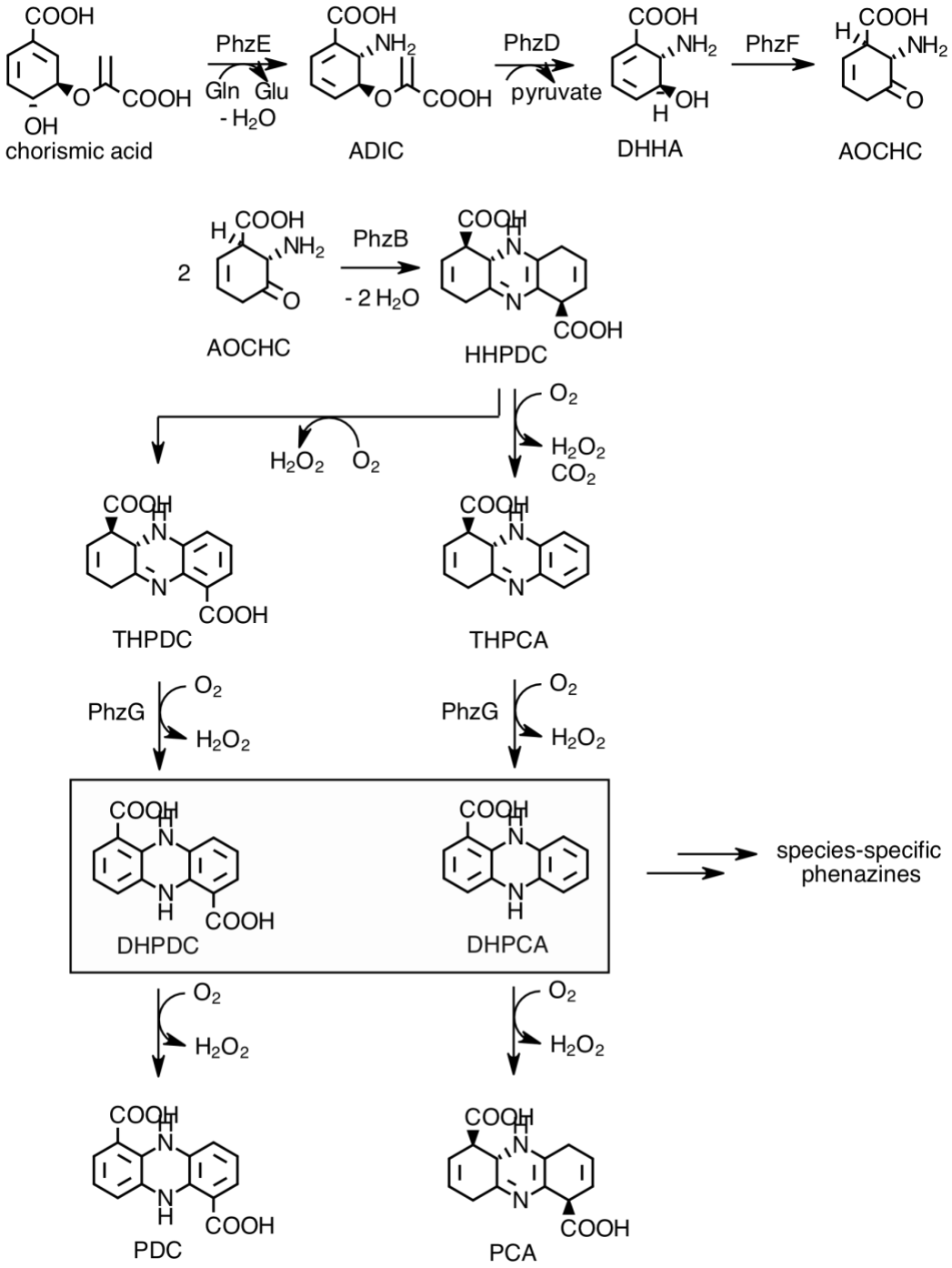

Figure 2. Current understanding of the biosynthesis of phenazine tricycle and species-specific phenazine derivatives from chorismic acid. The scheme was adopted with modifications from Guttenberger et al. (2017). ADIC, 2-amino-2-deoxyisochorismic acid; DHHA, trans-2,3-dihydro-3-hydroxyanthranilic acid; AOCHC, 6-amino-5-oxocyclohex-2-ene-1-carboxylic acid; HHPCD, hexahydrophenazine-1,6-dicarboxylic acid; THPDC, tetrahydrophenazine-1,6-dicarboxylic acid; THPCA, tetrahydrophenazine-1,6-carboxylic acid; DHPDC, 5,10-dihydro-PDC; DHPCA, 5,10-dihydro-PCA; PDC, phenazine-1,6-dicarboxylic acid; PCA, phenazine-1-carboxylic acid.

reaction is provided by glutamine. The conversion of chorismic acid to phenazines requires the concerted action of enzymes encoded by six “core biosynthesis” genes (Mavrodi et al., 2006). The initial biosynthetic steps are catalyzed by PhzE and involve the transformation of chorismic acid to 2-amino-2-deoxyisochorismic acid (ADIC), then the isochorismatase PhzD subsequently transforms ADIC to trans-2,3-dihydro-3-hydroxyanthranilic acid (DHHA). The DHHA is isomerized by PhzF, yielding a precursor that is condensed in a head-to-tail manner by PhzB, a small ketosteroid isomerase protein. Final steps in the core biosynthesis are catalyzed by the flavin-dependent PhzG and, depending on the bacterial species, result in phenazine-1-carboxylic acid or a mixture of the latter with phenazine-1,6-dicarboxylic acid (PDC). Many phenazine producers carry additional genes involved in further modification of PCA and/or PDC via hydroxylation, methylation, N-oxidation, prenylation, or glycosylation. Actinobacteria produce the most structurally complex phenazines, and their biosynthesis clusters often contain dozens of specialized modifying genes (Guttenberger et al., 2017). In addition to genetic and biochemical determinants, the spectrum and relative amounts of phenazines produced by a given species change in response to nutrients and environmental conditions (Peng et al., 2018).

Biological function of microbial phenazines

Although initially described as colorful bacterial pigments, phenazines later emerged as key contributors to numerous aspects of the biology of their producers (Price-Whelan et al., 2006). Phenazines generate oxygen radicals from the reduction of molecular oxygen due to their function as electron shuttles; as a result, they exhibit broad

antimicrobial properties. Simple phenazines synthesized by beneficial strains of *Pseudomonas* spp. in the plant rhizosphere suppress soilborne diseases caused by fungal pathogens (Chin-A-Woeng et al., 2003). Studies in aminal models revealed the critical contribution of pyocyanin (Figure 1) to lung infections by *Pseudomonas aeruginosa* (Lau et al., 2004). Similarly, this phenazine compound exists in high concentrations in cystic fibrosis patients (Wilson et al., 1988). Phenazine-producing strains of *P. fluorescens* and *P. aureofaciens* are more competitive plant colonizers and out-compete mutants that do not produce phenazines (Mazzola et al., 1992). Similarly, pyocyanin-deficient variants of *P. aeruginosa* were less virulent in mouse pneumonia infections (Lau et al., 2004). Some phenazines produced by *Streptomyces* and other actinomycetes exhibit low cytotoxicity and are studied as potential anti-infective or antitumor drugs (Laursen & Nielsen, 2004).

The electron-shuttling action of phenazines aids the survival of aerobic species in low-oxygen conditions by allowing them to maintain a sufficient electron gradient between the cell and its environment (Ciemniecki & Newman, 2020). Since mature biofilms create hypoxic conditions, phenazines hold particular relevance to biofilm formation (Dietrich et al., 2008). Also, the presence of redox-active phenazines promotes the reduction of minerals in phenazine producers (Hernandez et al., 2004). This process may benefit phenazine-producing bacteria by reducing ferric hydroxides to more soluble and biologically available ferrous iron (Wang et al., 2011).

Phenazine production in Enterobacterales

Phenazine production in enteric bacteria was first reported in *Pantoea agglomerans* Eh1087, which belongs to a group of enterobacteria that include insect

endosymbionts and plant pathogens capable of causing disease on a variety of plant species (Adeolu et al., 2016). The phenazine antibiotic AGA (Figure 1) produced *in planta* by *P. agglomerans* contributed to the bacterium's suppression of *Erwinia amylovora*, the causative agent of fireblight disease of apples and other plants of the *Rosacea* family (Giddens et al., 2003). The phenazine biosynthetic locus of Eh1087 consists of 16 genes, five of which (*ephA-E*) are engaged in the core biosynthesis and conversion of shikimic acid to PCA and PDC. The rest of the genes control further modifications of PDC to griseoluteic acid and AGA (Giddens et al., 2002). The Eh1087 phenazine cluster also encodes a phenazine-binding resistance protein and an efflux transporter. In addition to *P. agglomerans*, phenazine gene clusters were identified in several *Pectobacterium* spp., which are necrotrophic bacterial plant pathogens that cause soft rots and wilts of crop and ornamental plants (Li et al., 2018). However, that study focused primarily on comparative genome analysis and did not provide details regarding the organization and possible function of *Pectobacterium* phenazine genes.

CHAPTER III: MATERIALS AND METHODS

Strains used in this study

Bacterial strains used in this project include *Pectobacterium betavasculorum* Ecb168 (Axelrood et al., 1988), a sugar beet isolate from Monterey, CA, and *P. carotovorum* cc303 (Bull et al., 1994), a soil isolate from Oregon. Both strains were cultured for 48 h at 27°C in Tryptic Soy broth (Difco), and high molecular weight samples of their DNA were prepared using the cetyltrimethylammonium bromide method (Ausubel et al., 2002).

Sequencing, assembly, annotation, and analysis of bacterial genomes

Genomes of strains Ecb168 and cc303 were sequenced by the Texas A&M AgriLife Genomics and Bioinformatics Service (College Station, TX). Raw sequence reads were generated with a MiSeq instrument (Illumina, San Diego, CA), trimmed and clipped with Trim Galore v.0.6.1 (Krueger, 2015), and assessed for quality before assembly with the FastQC toolkit (Andrews, 2010). The filtered reads were assembled with Unicycler v.0.4.8 (Wick et al., 2017) and annotated with the RASTtk (Rapid Annotation using Subsystem Technology) annotation engine (Brettin et al., 2015) implemented in the Pathosystems Resource Integration Center (PATRIC) (Wattam et al., 2014). Contigs containing phenazine biosynthesis clusters were extracted from assemblies and processed for further analyses with Geneious Prime 2021 (Biomatters, Auckland, New Zealand).

Identification of phenazine biosynthesis genes in publicly available Enterobacterales genomes

DNA sequences of *Enterobacterales* phenazine clusters were acquired by basic local alignment search tool (BLAST) searches of bacterial genomes deposited in the NCBI GenBank (Benson et al., 2014). The screen was conducted with a tblastn search of genomic databases by their translated proteins using BLAST v2.10.1 (Camacho et al., 2009) and a cut-off e-value of 1e-5. The protein sequence of PhzA/B from *P. agglomerans* Eh1087 was selected as the target for database searches to identify *Enterobacterales* spp. with phenazine biosynthesis pathways. The analysis of core biosynthetic, putative modifying, and resistance genes was conducted in Geneious Prime 2021.

Comparative analysis of phenazine gene clusters

Inferred phylogenies of *Enterobacterales* were developed from core *phz* proteins in order to analyze the evolution of phenazine biosynthesis pathways. Amino acid sequences were concatenated and aligned with multiple sequence comparison by log-expectation (MUSCLE) (Edgar, 2004). Bootstrapped neighbor joining (NJ) phylogenies were constructed in Geneious Prime 2021 using protein distances corrected by the Jukes-Cantor model of evolution (Jukes & Cantor, 1969). The whole-genome maximum likelihood phylogenies were constructed using the Codon Tree algorithm in PATRIC (Wattam et al., 2014). The analysis was based on 50 shared single-copy genes identified by PGFams. The resultant bootstrapped phylogenies were exported for final formatting and editing to Geneious Prime 2021.

Distinct types of gene arrangement in phenazine clusters were identified by aligning nucleotide sequences in Geneious with multiple alignment using fast fourier transform (MAFFT) 7.309 (Katoh & Standley, 2013) and comparing the resultant % nucleotide identity patterns using heatmaps created in Morpheus (https://software.broadinstitute.org/morpheus/). Homologous phenazine biosynthesis genes and their functions were identified by multiway BLASTp searches in PATRIC (Wattam et al., 2014) with an E-value cutoff of 1e-06, identity of 40%, and coverage of 60%. Venn diagrams were generated using an online tool developed by the University of Ghent Bioinformatics & Evolutionary Genomics group (http://bioinformatics.psb.ugent.be/webtools/Venn/).

Genomic islands (GEs) containing phenazine genes were identified with the IslandViewer4 pipeline (Dhillon et al., 2015). This pipeline predicts horizontally transferred genome regions based on atypical codon usage (SIGI-HMM algorithm) (Waack et al., 2006) or sequence composition biases and hidden Markov model (HMM) profiles for mobility genes (IslandPath-DIMOB algorithm) (Bertelli & Brinkman, 2018). Putative GEs were manually examined in Geneious Prime 2021 to identify transposase pseudogenes and potential attachment sites.

CHAPTER IV: RESULTS

Genome sequences of *P. betavasculorum* Ecb168 and *P. carotovorum* cc303

The sequencing of the *P. betavasculorum* Ecb168 genome produced 2,565,614 high quality paired end reads, which totaled 632,844,887 bp. The assembly with Unicycler produced 68 contigs with a median coverage of 135× and N_{50} of 215,011 bp and N_{max} of 584,537 bp (Table 1). The Ecb168 chromosome was 4,688,175-bp long with a G+C content of 50.9%. The genome contained 4,5743 protein-coding genes and 69 RNA genes. The annotation revealed 1,206 proteins with Enzyme Commission (EC) numbers, 915 proteins with Gene Ontology (GO) terms, and 909 hypothetical or conserved hypothetical proteins. Further genome analysis revealed the presence of PhzA/B, PhzD, PhzE, PhzF, and PhzG core biosynthesis genes. The genomes also encoded 43 genes associated with drug resistance, including several multidrug efflux systems (EmrAB-OMF, MdtABC-TolC, AcrAB-TolC, AcrAD-TolC). A total of 45 genes were flagged by PATRIC as potentially encoding virulence factors. The genome also encoded three clustered regularly interspaced short palindromic repeat (CRISPR) arrays with 53 repeats and 49 spacers.

For *P. carotovorum* cc303, the sequence run produced 2,312,787 high quality paired end reads totaling 570,131,826 bp. The final assembly had 89 contigs with a median coverage of 118×, N_{50} of 130,797 bp, and N_{max} of 493,732 bp (Table 1). The resultant 4,830,768-bp long genome had a G+C content of 51.0% and contained 68 RNA- and 4,776 protein-coding genes. Putative functions were assigned to 3,347 genes, 1,194 of which encoded proteins with EC numbers. A total of 896 genes encoded proteins with GO assignments, while 1,124 genes were annotated as hypothetical. A total of 46 genes

were identified as potential virulence factors, and 48 were associated with drug resistance. The sequenced genome also encoded a CRISPR array with 14 repeats and 13 spacers.

The distribution of phz genes among major clades of Enterobacterales

Screening of publicly accessible databases yielded multiple *Enterobacterales* genomes carrying phenazine biosynthesis genes. Including *P. betavasculorum* Ecb168 and *P. carotovorum* cc303, phenazine biosynthesis pathways were identified in 46 strains representing nine genera and at least 14 different species (Figure 3). According to GenBank, these strains were of worldwide origin and came from North (Canada, Mexico, USA) and South America (Brazil), Europe (Belarus, Finland, France, Germany, Portugal, Russia, United Kingdom), Africa (Egypt, Tanzania), Asia (China, Pakistan, South Korea, Vietnam), and New Zealand. The whole genome phylogeny based on 50 shared single-copy genes revealed that the putative Phz+ producers collectively represented five out of seven major *Enterobacterales* clades (Adeolu *et al*., 2016). Strains carrying phenazine biosynthesis genes were particularly abundant in *Enterobacter-Escherichia* and *Pectobacterium-Dickeya* clades, which encompass numerous economically important animal and plant pathogens.

Table 1. Genome features of strains *P. betavasculorum* Ecb168 and *P. carotovorum* cc303.

Strain	Fold coverage	Genome size (bp)	No. of contigs	N_{50} values (bp)	G+C (%)	Total no. of genes	No. of RNA genes	Total no. of CDSs[a]	No. of proteins with ECs[b]	No. of proteins with GO terms[c]	No. of hypothetical proteins
Ecb168	135×	4,688,175	68	215,011	50.9	4,643	69	4,574	1,206	915	909
cc303	118×	4,830,768	89	130,797	51	4,844	68	4,776	1,194	896	1,124

[a] CDSs, coding sequences. [b] ECs, Enzyme Commission numbers. [c] Proteins with Gene Ontology (GO) assignments.

Enterobacterales carry several distinct types of phenazine clusters

The visual examination of phenazine clusters revealed several distinct sets and organization patterns of *phz* genes. To sort the *Enterobacterales* phenazine clusters into distinct groups, their DNA sequences were aligned with MAFFT (Katoh & Standley, 2013) and the resultant pairwise percent nucleotide identity values were visualized as a heatmap. The analysis revealed that *phz* pathways form six clearly defined clusters (Figure 4). Cluster I contained sequences from *Enterobacter* and *Klebsiella*, cluster II contained *phz* genes from *Escherichia*, *Providencia*, and *Serratia*, cluster III was comprised of *phz* genes from different species of *Pectobacterium*, cluster IV contained sequences from *Xenorhabdus* and *Photorhabdus*, while cluster V contained *Pantoea* and *Pectobacterium*. Finally, the smallest cluster VI contained distinct phenazine genes from strains *Xenorhabdus japonica* DSM 16522 and *Xenorhabdus vietnamensis* DSM 22392.

Next, we conducted a series of comparative analyses using six strains selected as typical representatives of the six distinct clusters shown in Figure 4. These representative strains included *Klebsiella pneumoniae* 44825 (cluster I), *E. coli* M15 (cluster II), *P. betavasculorum* Ecb168 (cluster III), *X. nematophila* SII (cluster IV), *P. carotovorum* cc303 (cluster V), and *X. vietnamensis* DSM 22392 (cluster VI). Protein sequences encoded by the *phz* cluster of each strain were compared by multiway BLASTp analysis (cutoff parameters of E-value = e-06, 40% identity, 60% coverage). The resultant BLAST hits were summarized in the form of a Venn diagram (Figure 5).

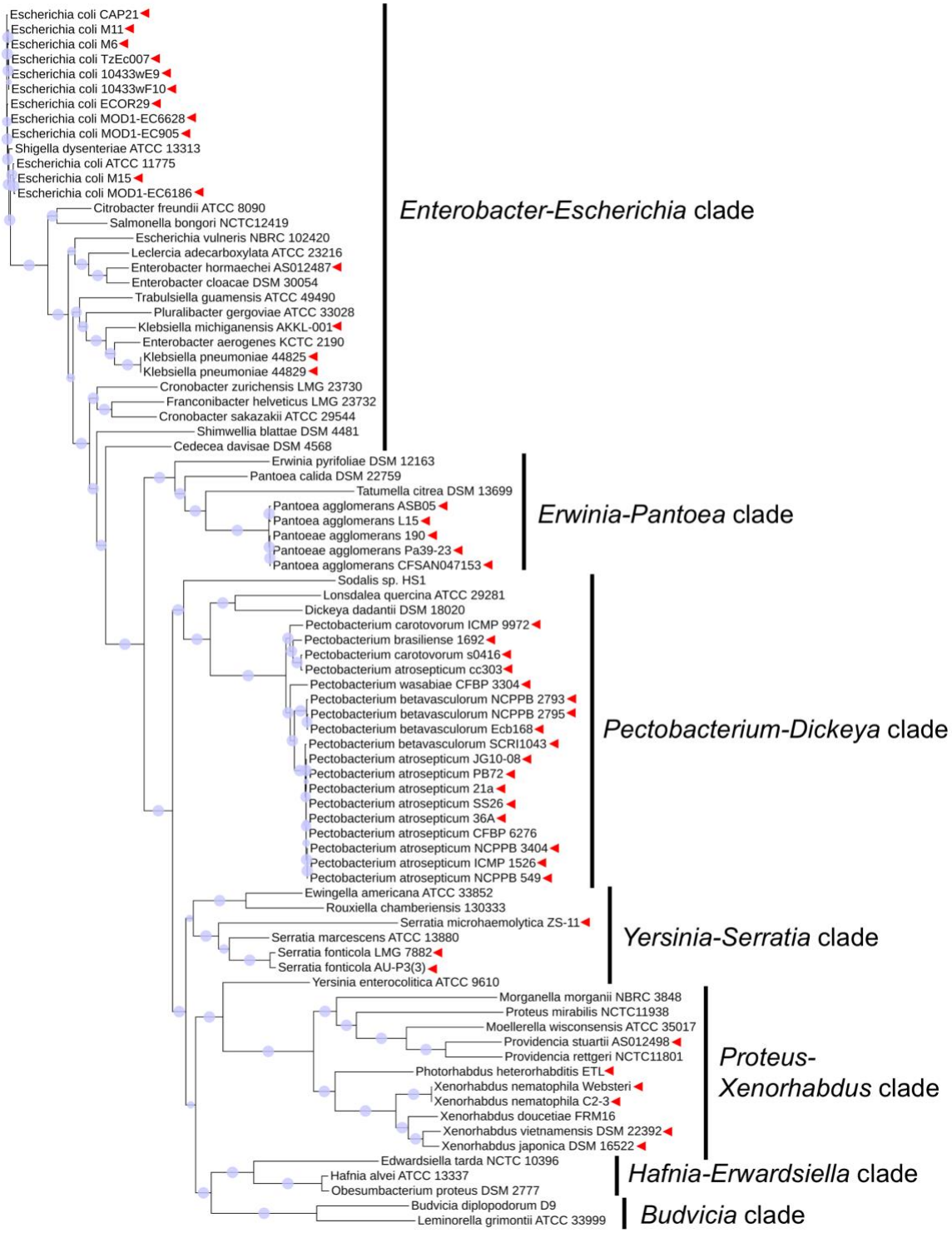

Figure 3. Whole genome-based phylogeny of Enterobacterales. The distribution of phenazine biosynthesis genes among different clade of the order in indicated by red triangles. The whole-genome maximum likelihood phylogenies were constructed using the Codon Tree method in PATRIC (Wattam et al., 2014). Circles on the tree nodes indicate bootstrap values that vary between 50.0% (smallest circle) and 100% (largest circles). The final tree was visualized in iTOL (Letunic & Bork, 2016).

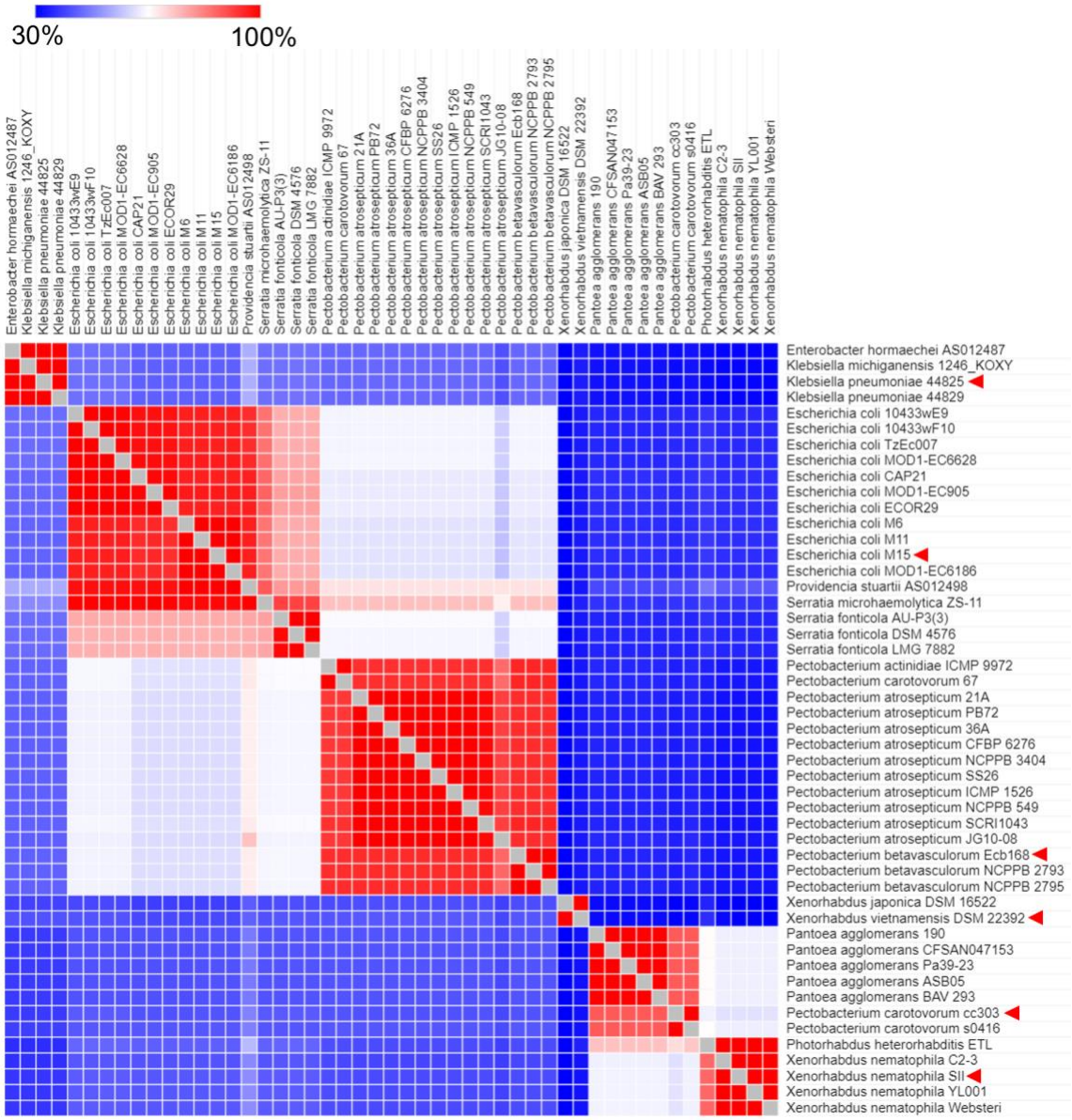

Figure 4. Heatmap of percent nucleotide identity values among phenazine loci identified in Enterobacterales genomes. DNA sequences of phenazine clusters were aligned in Geneious Prime with MAFFT (Katoh & Standley, 2013) and the resultant % nucleotide identity matrix was used to generate a heatmap in Morpheus (https://software.broadinstitute.org/morpheus/). Red arrows indicate six species chosen for further analyses as representatives of distinct clusters.

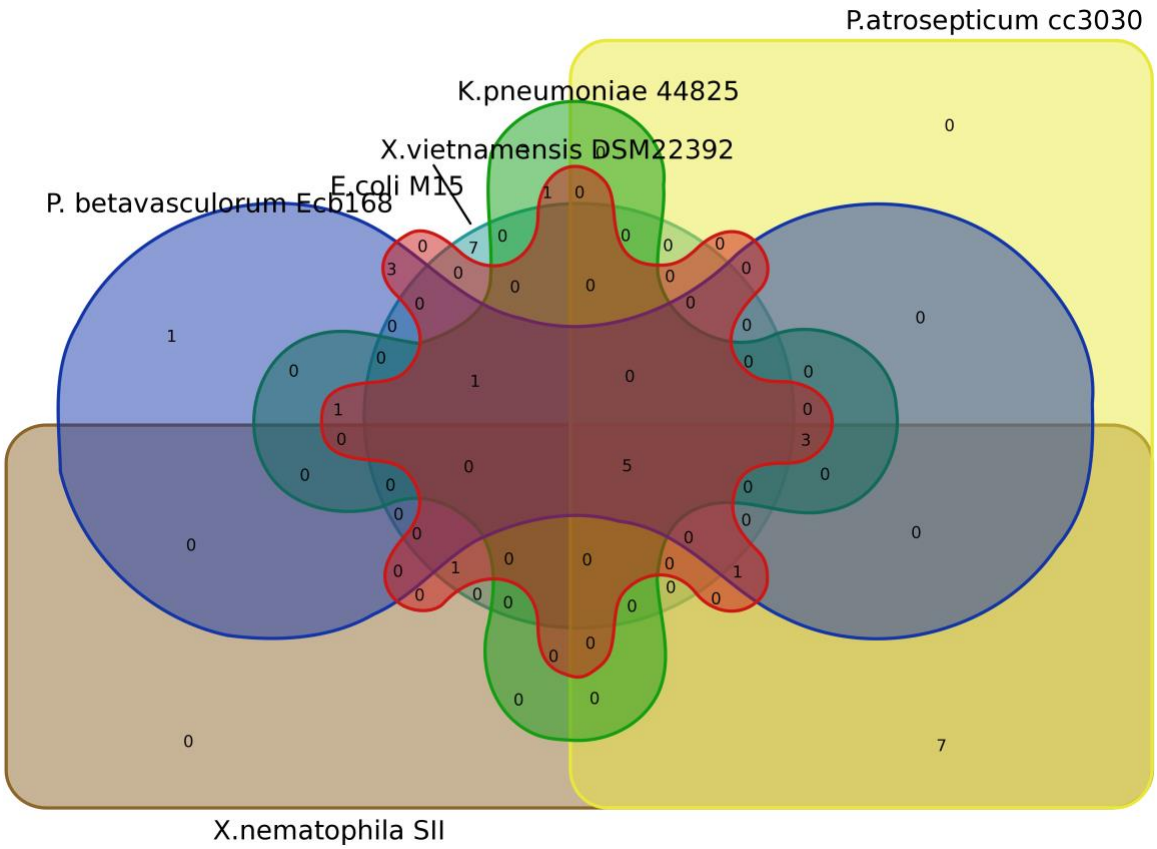

Figure 5. Venn diagram showing unique and homologous genes in phenazine biosynthesis pathways of P. betavasculorum Ecb168, P. carotovorum cc303, K. pneumoniae 44825, E. coli M15, X. nematophila SII, and X. vietnamensis DSM 22392. The list of genes used in this analysis and their predicted functions are provided in Table 3.

Results of the analysis revealed that the compared phenazine loci were similar in size but contained a very diverse gene set. The individual *phz* pathways had between 14 and 17 genes, but only five of them were shared by all six representative strains. These common genes encoded the core biosynthetic enzymes PhzA/B, PhzD, PhzE, PhzF, and PhzG (Table 2). The distribution of other genes varied, although a significant overlap was detected between gene sets of

Table 2. The list of genes and function encoded by phenazine biosynthesis clusters of Enterobacterales. Homologous genes identified by multiway BLASTp searches are listed in rows. Different functional gene categories are indicated with color as follows: red – core phenazine biosynthesis enzymes, lime green – enzymes involved in the modification of phenazine tricycle, orange – resistance to phenazines, blue – regulation.

Predicted function	Gene	Genome locus tag					
		***P. betavasculorum* Ecb168**	***E. coli* M15**	***K. pneumoniae* 44825**	***P. carotovorum* cc3030**	***X. nematophila* SII**	***X. vietnamensis* DSM 22392**
phenazine-binding protein	*ehpR*	SEED:fig|554.7.peg.1615	RG61_RS04660		RAST2:fig|29471.81.peg.4613	H8F46_RS01280	
SDR family NAD(P)-dependent oxidoreductase	*ehpK*	SEED:fig|554.7.peg.1614	RG61_RS04665	EF509_RS05710	RAST2:fig|29471.81.peg.4623	H8F46_RS01330	
ketosteroid isomerase-related protein	*phzA/B*	SEED:fig|554.7.peg.1613	RG61_RS04670	EF509_RS05715	RAST2:fig|29471.81.peg.4614	H8F46_RS01285	Xvie_RS01900
isochorismatase	*phzD*	SEED:fig|554.7.peg.1612	RG61_RS04675	EF509_RS05720	RAST2:fig|29471.81.peg.4615	H8F46_RS01290	Xvie_RS01905
phenazine biosynthesis protein phzE	*phzE*	SEED:fig|554.7.peg.1611	RG61_RS04680	EF509_RS05725	RAST2:fig|29471.81.peg.4616	H8F46_RS01295	Xvie_RS01910
hypothetical protein		SEED:fig|554.7.peg.1610	RG61_RS04685	EF509_RS05730			Xvie_RS01915
trans-2,3-dihydro-3-hydroxyanthranilate isomerase	*phzF*	SEED:fig|554.7.peg.1609	RG61_RS04690	EF509_RS05735	RAST2:fig|29471.81.peg.4617	H8F46_RS01300	Xvie_RS01920
pyridoxal 5'-phosphate synthase	*phzG*	SEED:fig|554.7.peg.1608	RG61_RS04695	EF509_RS05740	RAST2:fig|29471.81.peg.4618	H8F46_RS01305	Xvie_RS01925
acyl-CoA synthase of ANL superfamily	*ehpF*	SEED:fig|554.7.peg.1607	RG61_RS04700	EF509_RS05745	RAST2:fig|29471.81.peg.4619	H8F46_RS01310	
phenazine biosynthesis protein EhpG	*ehpG*	SEED:fig|554.7.peg.1606	RG61_RS04705	EF509_RS05750	RAST2:fig|29471.81.peg.4620	H8F46_RS01315	
polyketide synthase		SEED:fig|554.7.peg.1605	RG61_RS04710	EF509_RS05755			
non-ribosomal peptide synthase		SEED:fig|554.7.peg.1604	RG61_RS04715				
hypothetical protein		SEED:fig|554.7.peg.1603	RG61_RS28735				
FAD-dependent oxidoreductase		SEED:fig|554.7.peg.1602	RG61_RS04725				
PQQ-dependent aldose sugar dehydrogenase		SEED:fig|554.7.peg.1601					
3-deoxy-7-phospho heptulonate synthase	*phzC*		RG61_RS04730			H8F46_RS01360	Xvie_RS01930
SAM-dependent methyltransferase	*ehpI*				RAST2:fig|29471.81.peg.4621	H8F46_RS01320	

Table 2 (continued)

MFS drug efflux transporter	*ehpJ*			RAST2:fig|29471.81.peg.4622	H8F46_RS01325	
hypothetical protein	*ehpL*			RAST2:fig|29471.81.peg.4624	H8F46_RS01335	
long-chain-fatty-acid-CoA ligase	*ehpM*			RAST2:fig|29471.81.peg.4625	H8F46_RS01340	
hypothetical protein	*ehpN*			RAST2:fig|29471.81.peg.4626	H8F46_RS01345	
hypothetical protein	*ehpO*			RAST2:fig|29471.81.peg.4627	H8F46_RS01350	
hypothetical protein				RAST2:fig|29471.81.peg.4628	H8F46_RS01355	
redox-sensitive transcriptional activator SoxR						Xvie_RS01935
monooxygenase						Xvie_RS01880
RNA polymerase sigma factor						Xvie_RS01885
NAD(P)/FAD-dependent oxidoreductase						Xvie_RS01895
FAD-dependent monooxygenase						Xvie_RS01890
RND efflux transporter, periplasmic subunit						Xvie_RS01940
RND efflux transporter, permease subunit						Xvie_RS01945
4'-phosphopantetheinyl transferase superfamily protein			RG61_RS04735	EF509_RS05775		
alpha/beta fold hydrolase				EF509_RS05770		
hypothetical protein				EF509_RS05765		
HAD-IIIC family phosphatase				EF509_RS05760		

P. betavasculorum Ecb168 and *E. coli* M15, as well as between *P. carotovorum* cc303 and *X. nematophila* SII (Figure 5, Table 2). The highest proportion of unique genes was observed in the phenazine locus of *X. vietnamensis* DSM 22392. In addition to core biosynthesis, the analyzed pathways included diverse genes involved in the creation of more complex phenazines, as well as genes predicted to function in regulation and resistance to phenazines (Table 2).

Evidence for horizontal gene transfer in phenazine clusters of Enterobacterales

The evolutionary history of phenazine genes in *Enterobacterales* was explored by constructing and comparing protein-based whole-genome phylogenies with phylogenies based on the concatenated amino acid sequences of shared core biosynthesis genes. Although most taxa clustered consistently in both analyses, we observed a number of important discrepancies (Figure 6). For example, phenazine genes of *S. fonticola* and *S. microhaemolytica* formed a well-supported clade with their homologs from *E. coli*, although these organisms belong to two distinct clades of *Enterobacterales*. Similarly, *phz* genes of *P. agglomerans*, *P. carotovorum* cc303, *P. polaris* s0416, *Xenorhabdus*, and *Photorhabdus* clustered together, while in the whole-genome phylogeny these organisms belonged to different clades. Other examples of incongruent clustering patterns included *K. pneumoniae* 44825 and 44829, *K. michiganensis* 1246-KOXY, *Enterobacter hormaechei* AS012487, *X. japonica* DSM 16522, and *X. vietnamensis* DSM 22392 (Figure 6).

We further screened genome regions flanking phenazine loci in different *Enterobacterales* for the presence of features commonly associated with mobile genetic

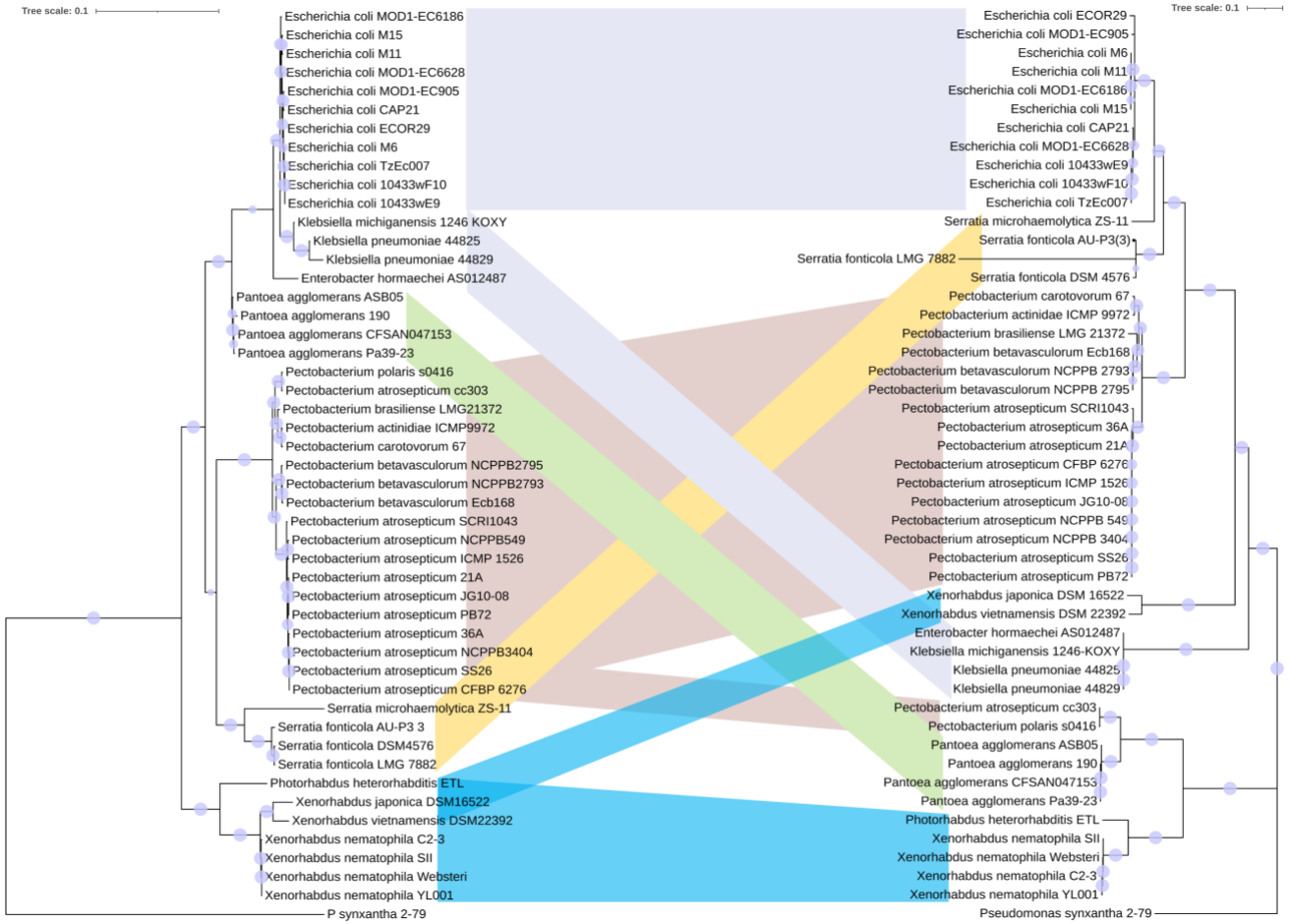

Figure 6. Comparison of the protein-based whole genome phylogeny of Enterobacterales (left) to that based on concatenated amino acid sequences of PhzA/B, PhzD, PhzE, and PhzG (right). The whole-genome maximum likelihood phylogeny was constructed using the Codon Tree function of PATRIC (Wattam et al., 2014). The neighbor-joining phylogeny of core phenazine biosynthesis genes is based on protein sequences aligned with MUSCLE (Edgar, 2004) and Jukes-Cantor distances (Jukes & Cantor, 1969). Sequences from *P. synxantha* 2-79 were used as an outgroup. Circles indicate bootstrap values over 60%. Both trees were edited in iTOL (Letunic & Bork, 2016). Scale bars indicate substitution per site.

Table 3. Mobile genetic elements (MGEs) associated with phenazine biosynthesis clusters in *Enterobacterales*.

Reference strain	Locus tag range	Size (bp)	G+C (%)	Integrase	tRNA	MGE type	Notable features	Strains with similar MGEs
E. coli M15	RG61_RS04365 to RG61_RS04805	87,460	50.4	Yes	Yes, $tRNA^{Phe}$	ICE	Type IV secretion system (mating pair formation, DNA transfer and replication genes), transposases, high HHR[a]. Cargo genes encode a toxin-antitoxin system, a hemolysin, phenazine pathway.	*E. coli* M6, *E. coli* M11, *E. coli* MOD1-EC6186, *E. coli* MOD1-EC6628, *E. coli* ECOR29, *S. fonticola* LMG 7882, *S. fonticola* AU-P3(3), *S. fonticola* DSM 4576, *P. heterorhabditis* ETL
K. pnemoniae 44825	EF509_RS05670 to EF509_RS06190	94,471	58.5	Yes	Yes, $tRNA^{Gly}$	ICE	Type IV secretion system (mating pair formation, DNA transfer and replication genes), transposases, high HHR[a]. Cargo genes encode toxin-antitoxin systems, an ABC family transporter, a group II intron reverse transcriptase, phenazine pathway.	*K. pneumoniae* 44829, *E. hormaechei* AS012487
P. agglomerans CFSAN047153	D1628_RS22090 to D1628_RS24570	211,326	51.9	Yes	No	Plasmid	Plasmid replication genes, transposases, high HHR[a]. Cargo genes encode toxin-antitoxin systems, type I fimbriae, LPS modification enzymes, drug efflux transporters, transcription factors, GGDEF and EAL domain proteins, *phz* pathway.	*P. agglomerans* ASB05, *P. agglomerans* BAV293, *P. agglomerans* 190, *P. agglomerans* Pa39-23
X. nematophila SII	H8F46_RS01180 to H8F46_RS01380	44,362	43.7	Yes	Yes, $tRNA^{Phe}$	Genomic island	Transposases, high HHR. Cargo genes encode an N-6 DNA methylase, a type I restriction-modification system, a TraI domain protein, *phz* pathway.	*X. nematophila* YL001

[a] HHR, high ratio of hypothetical proteins.

elements (MGEs). The screen revealed MGEs in almost half of the studied genomes, in which *phz* clusters formed parts of four distinct types of MGEs (Table 3). Strains of *E. coli*, *S. fonticola*, *S. microhaemolytica*, and *Photorhabdus heterorhabditis* carried an 87-kb integrative and conjugative element (ICE) integrated into $tRNA^{Phe}$. A slightly different 94-kb ICE was integrated into $tRNA^{Gly}$ of *K. pneumoniae* 44825, *K. pneumoniae* 44829, and *E. hormaechei* AS012487. In addition to *phz* pathways, both types of ICE elements harbored site-specific integrases, components of type IV secretion machinery, and various cargo genes. In *X. nematophila* SII and *X. nematophila* YL001, phenazine genes formed part of a 44-kb genomic island integrated into $tRNA^{Phe}$. Finally, in *P. agglomerans* strains CFSAN047153, ASB05, BAV293, 190, and Pa39-23, phenazine gene clusters were located on a 211-kb plasmid.

CHAPTER V: DISCUSSION

The results of this study demonstrated that phenazine biosynthesis genes are ubiquitously distributed across several clades of *Enterobacterales*. These genes are arranged into several types of *phz* clusters that share five core biosynthesis genes, *phzA/B*, *phzD*, *phzE*, *phzF*, and *phzG*, that encode enzymes essential to the assembly of the core phenazine structure (Figure 5, Table 2). The variable presence of another core biosynthesis gene, *phzC*, may reflect differences in the level of phenazines produced by individual groups of *Enterobacterales*. In contrast to the conserved core biosynthesis functions, genes encoding enzymes involved in the modification of the phenazine tricycle were numerous and diverse. Bacterial species with phenazine pathways exemplified by *P. carotovorum* cc303 and *X. nematophila* SII carry biosynthesis genes similar to the well-studied strain *P. agglomerans* Eh1087 (Giddens et al., 2002). They are predicted to produce phenazine-1,6-dicarboxylic acid and convert it to D-alanylgriseoluteic acid (AGA). The diversity and identity of phenazine compounds produced by other groups of *Enterobacterales* cannot be deduced through the comparison of gene sequences and will require instrumental analysis of members of those groups.

The comparative analysis revealed that in almost half of the analyzed genomes, *phz* genes were associated with genomic islands, integrative conjugative elements, and plasmids (Table 3). These results suggest that in *Enterobacterales*, *phz* pathways are disseminated via active horizontal gene transfer. This is in contrast to other groups of bacteria, such as *Pseudomonas*, where phenazine biosynthesis genes represent part of the core microbiome and are tightly integrated into the metabolism and regulated via quorum sensing. In addition to phenazine biosynthesis genes, the mobile genetic elements

identified in this study contain cargo genes that encode toxin-antitoxin systems, transporters, surface appendages, DNA modification enzymes, regulatory proteins, and virulence factors. These genes likely confer multiple and diverse phenotypes to host cells and may play an important role in the evolution of *Enterobacterales* (Johnson & Grossman, 2015).

Our results also pose a question about the role of phenazines in the biology of *Enterobacterales*. We hypothesize that these secondary metabolites function primarily as antibiotics that help the producing strains to outcompete other bacteria in their ecological niche. An example of such interspecies competition is *P. agglomerans* Eh1087, which suppresses phytopathogen *Erwinia amylovora* by secreting the phenazine antibiotic D-alanylgriseoluteic acid (Giddens et al., 2003). To neutralize the toxicity of phenazines, *P. agglomerans* Eh1087 uses the EhpR protein that binds D-alanylgriseoluteic acid and delivers it to the efflux transporter EhpJ (Yu et al., 2011). Our analysis revealed that in almost all *Enterobacterales*, phenazine pathways also contain homologs of EhpR and/or putative drug efflux transporters (Table 2). In the opportunistic human pathogen *Pseudomonas aeruginosa*, the phenazine metabolite pyocyanin acts as a conserved virulence factor in mammals (Hall et al., 2016), invertebrates like *Drosophila melanogaster* (Lau et al., 2003) and *Caenorhabditis elegans* (Mahajan-Miklos et al., 1999), and even plants (Rahme et al., 2000). Among *Enterobacterales* carrying phenazine genes are several important plant pathogens (*Pectobacterium atrosepticum*, *P. betavasculorum*, *P. carotovorum*) and opportunistic pathogens of humans and animals (*E. coli*, *Klebsiella pneumoniae*, *Serratia fonticola*). Although it is possible that the

phenazines of *Enterobacterales* also act as virulence factors, the identification of their function will require laboratory experiments.

REFERENCES

Adeolu M, Alnajar S, Naushad S, S Gupta R. 2016. Genome-based phylogeny and taxonomy of the *'Enterobacteriales'*: proposal for *Enterobacterales* ord. nov. divided into the families *Enterobacteriaceae*, *Erwiniaceae* fam. nov., *Pectobacteriaceae* fam. nov., *Yersiniaceae* fam. nov., *Hafniaceae* fam. nov., *Morganellaceae* fam. nov., and *Budviciaceae* fam. nov. Int. J. Syst. Evol. Microbiol. 66: 5575–5599

Andrews S. 2010. FastQC: a quality control tool for high throughput sequence data. Available online at: http://www.bioinformatics.babraham.ac.uk/projects/fastqc

Arkin AP, Cottingham RW, Henry CS, Harris NL, Stevens RL, Maslov S, Dehal P, Ware D, Perez F, Canon S, Sneddon MW, Henderson ML, Riehl WJ, Murphy-Olson D, Chan SY, Kamimura RT, Kumari S, Drake MM, Brettin TS, Glass EM, Chivian D, Gunter D, Weston DJ, Allen BH, Baumohl J, Best AA, Bowen B, Brenner SE, Bun CC, Chandonia JM, Chia JM, Colasanti R, Conrad N, Davis JJ, Davison BH, DeJongh M, Devoid S, Dietrich E, Dubchak I, Edirisinghe JN, Fang G, Faria JP, Frybarger PM, Gerlach W, Gerstein M, Greiner A, Gurtowski J, Haun HL, He F, Jain R, et al. 2018. KBase: The United States Department of Energy Systems Biology Knowledgebase. Nat. Biotechnol. 36: 566–569

Ausubel FM, Brent R, Kingston RE, Moore DD, Seidman JG, Smith JA, Struhl K. 2002. Short Protocols in Molecular Biology, 5th ed. John Wiley and Sons, New York, NY.

Axelrood PE, Rella M, Schroth MN. 1988. Role of antibiosis in competition of *Erwinia* strains in potato infection courts. Appl. Environ. Microbiol. 54: 1222–1229

Benson DA, Clark K, Karsch-Mizrachi I, Lipman DJ, Ostell J, Sayers EW. 2014. GenBank. Nucleic Acids Res. 42: D32–D37

Bertelli C, Brinkman FSL. 2018. Improved genomic island predictions with IslandPath-DIMOB. Bioinformatics 34: 2161–2167

Biessy A, Novinscak A, Blom J, Léger G, Thomashow LS, Cazorla FM, Josic D, Filion M. 2019. Diversity of phytobeneficial traits revealed by whole-genome analysis of worldwide-isolated phenazine-producing *Pseudomonas* spp. Environ. Microbiol. 21: 437–455

Blackwood BP, Hunter CJ. 2016. *Cronobacter* spp. Microbiol Spectr. 4(2). doi: 10.1128/microbiolspec.EI10-0002-2015

Brettin T, Davis JJ, Disz T, Edwards RA, Gerdes S, Olsen GJ, Olson R, Overbeek R, Parrello B, Pusch GD, Shukla M, Thomason JA 3rd, Stevens R, Vonstein V, Wattam AR, Xia F. 2015. RASTtk: a modular and extensible implementation of the RAST algorithm for building custom annotation pipelines and annotating batches of genomes. Sci Rep. 5: 8365

Bull CT, Ishimaru CA, Loper JE. 1994. Two genomic regions involved in catechol siderophore production by *Erwinia carotovora*. Appl. Environ. Microbiol. 60: 662–669

Boucher HW, Talbot GH, Bradley JS, Edwards JE, Gilbert D, Rice LB, Scheld M, Spellberg B, Bartlett J. 2009. Bad bugs, no drugs: no ESKAPE! An update from the Infectious Diseases Society of America. Clin. Infect. Dis. 48: 1–12

Camacho C, Coulouris G, Avagyan V, Ma N, Papadopoulos J, Bealer K, Madden TL. 2009. BLAST+: architecture and applications. BMC Bioinformatics 10: 421

Chen IA, Chu K, Palaniappan K, Pillay M, Ratner A, Huang J, Huntemann M, Varghese N, White JR, Seshadri R, Smirnova T, Kirton E, Jungbluth SP, Woyke T, Eloe-

Fadrosh EA, Ivanova NN, Kyrpides NC. 2019. IMG/M v.5.0: an integrated data management and comparative analysis system for microbial genomes and microbiomes. Nucleic Acids Res. 47: D666–D677

Chin-A-Woeng TFC, Bloemberg GV, Lugtenberg BJJ. 2003. Phenazines and their role in biocontrol by *Pseudomonas* bacteria. New Phytol. 157: 503–502

Ciemniecki JA, Newman DK. 2020. The potential for redox-active metabolites to enhance or unlock anaerobic survival metabolisms in aerobes. J. Bacteriol. 202: e00797-19

Dar D, Thomashow LS, Weller DM, Newman DK. 2020. Global landscape of phenazine biosynthesis and biodegradation reveals species-specific colonization patterns in agricultural soils and crop microbiomes. eLife 9: e59726

Dhillon BK, Laird MR, Shay JA, Winsor GL, Lo R, Nizam F, Pereira SK, Waglechner N, McArthur AG, Langille MG, Brinkman FS. 2015. IslandViewer 3: more flexible, interactive genomic island discovery, visualization and analysis. Nucleic Acids Res. 43: W104–W108

Dietrich LE, Teal TK, Price-Whelan A, Newman DK. 2008. Redox-active antibiotics control gene expression and community behavior in divergent bacteria. Science 321: 1203–1206

Duszenko N, Buan NR. 2017. Physiological evidence for isopotential tunneling in the electron transport chain of methane-producing archaea. Appl. Environ. Microbiol. 83: e00950-17

Edgar RC. 2004. MUSCLE: multiple sequence alignment with high accuracy and high throughput. Nucleic Acids Res. 32: 1792–1797

Ferone M, Gowen A, Fanning S, Scannell AGM. 2020. Microbial detection and identification methods: Bench top assays to omics approaches. Compr. Rev. Food Sci. Food Saf. 19: 3106–3129

Giddens SR, Feng YJ, Mahanty HK. 2002. Characterization of a novel phenazine antibiotic gene cluster in *Erwinia herbicola* Eh1087. Mol. Microbiol. 45: 769–783

Giddens SR, Houliston GJ, Mahanty HK. 2003. The influence of antibiotic production and pre-emptive colonization on the population dynamics of *Pantoea agglomerans* (*Erwinia herbicola*) Eh1087 and *Erwinia amylovora* in planta. Env. Microbiol. 5: 1016–1021

Giddens SR, Feng YJ, Mahanty HK. 2002. Characterization of a novel phenazine antibiotic gene cluster in *Erwinia herbicola* Eh1087. Mol. Microbiol. 45: 769–783

Guttenberger N, Blankenfeldt W, Breinbauer R. 2017. Recent developments in the isolation, biological function, biosynthesis, and synthesis of phenazine natural products. Bioorg. Med. Chem. 25: 6149–6166

Hall S, McDermott C, Anoopkumar-Dukie S, McFarland AJ, Forbes A, Perkins AV, Davey AK, Chess-Williams R, Kiefel MJ, Arora D, Grant GD. 2016. Cellular effects of pyocyanin, a secreted virulence factor of *Pseudomonas aeruginosa*. Toxins (Basel). 8: 236

Hassan HM, Fridovich I. 1980. Mechanism of the antibiotic action of pyocyanine. J. Bacteriol. 141: 156–163

Hernandez ME, KapplerA, Newman DK. 2004. Phenazines and other redox-active antibiotics promote microbial mineral reduction. Appl. Environ. Microbiol. 70: 921–928

Johnson CM, Grossman AD. 2015. Integrative and conjugative elements (ICEs): what they do and how they work. Annu. Rev. Genet. 49: 13.1–13.25

Katoh K, Standley DM. 2013. MAFFT multiple sequence alignment software version 7: improvements in performance and usability. Mol. Biol. Evol. 30: 772–780

Korth H, Romer A, Budzikiewicz H, Pulverer G. 1978. 4,9-Dihydroxyphenazine-1,6-dicarboxylic acid dimethylester and the "missing link" in phenazine biosynthesis. J. Gen. Microbiol. 104: 299–303

Krueger F. 2015. Trim Galore: a wrapper tool around Cutadapt and FastQC to consistently apply quality and adapter trimming to FastQ files. http://www.bioinformatics.babraham.ac.uk/projects/trim_galore/

Lau GW, Ran H, Kong F, Hassett DJ, Mavrodi D. 2004. *Pseudomonas aeruginosa* pyocyanin is critical for lung infection in mice. Infect. Immun. 72: 4275–4278

Lau GW, Goumnerov BC, Walendziewicz CL, Hewitson J, Xiao W, Mahajan-Miklos S, Tompkins RG, Perkins LA, Rahme LG. 2003. The *Drosophila melanogaster* toll pathway participates in resistance to infection by the Gram-negative human pathogen *Pseudomonas aeruginosa*. Infect Immun. 71: 4059-4066

Laursen JB, Nielsen J. 2004. Phenazine natural products: Biosynthesis, synthetic analogues, and biological activity. Chem. Rev. 104: 1663–1685

Letunic I, Bork P. 2016. Interactive tree of life (iTOL) v3: an online tool for the display and annotation of phylogenetic and other trees. Nucleic Acids Res. 44: W242–245.

Li X, Ma Y, Liang S, Tian Y, Yin S, Xie S, Xie H. 2018. Comparative genomics of 84 *Pectobacterium* genomes reveals the variations related to a pathogenic lifestyle. BMC Genomics 19: 889

Liu GY, Nizet V. 2009. Color me bad: microbial pigments as virulence factors. Trends Microbiol. 17: 406–413

Mahajan-Miklos S, Tan MW, Rahme LG, Ausubel FM. 1999. Molecular mechanisms of bacterial virulence elucidated using a *Pseudomonas aeruginosa-Caenorhabditis elegans* pathogenesis model. Cell 96: 47-56

Mavrodi DV, Blankenfeldt W, Thomashow LS. 2006. Phenazine compounds in fluorescent *Pseudomonas* spp. biosynthesis and regulation. Annu. Rev. Phytopathol. 44: 417–445

Mavrodi DV, Bonsall RF, Delaney SM, Soule MJ, Phillips G, Thomashow LS. 2001. Functional analysis of genes for biosynthesis of pyocyanin and phenazine-1-carboxamide from *Pseudomonas aeruginosa* PAO1. J. Bacteriol. 183: 6454–6465

Mazzola M, Cook RJ, Thomashow LS, Weller DM, Pierson LS. 1992. Contribution of phenazine antibiotic biosynthesis to the ecological competence of fluorescent pseudomonads in soil habitats. Appl. Environ. Microbiol. 58: 2616–2624

Jukes TH, Cantor CR. 1969. Evolution of protein molecules. *In* Munro HN (ed), Mammalian Protein Metabolism, pp. 21–132, Academic Press, New York

Octavia S, Lang R. 2014. The family *Enterobacteriacea*. *In* Rosemberg E, De Long E, Lory S, Stackebrandt E, Thompson F (ed), The Prokaryotes, 4th edition, pp. 225–286, Springer-Verlag, Berlin

Peng H, Tan J, Bilal M, Wang W, Hu H, Zhang X. 2018. Enhanced biosynthesis of phenazine-1-carboxamide by *Pseudomonas chlororaphis* strains using statistical experimental designs. World J. Microbiol. Biotechnol. 34: 129

Price-Whelan A, Dietrich LE, Newman DK. 2006. Rethinking 'secondary' metabolism: physiological roles for phenazine antibiotics. Nat. Chem. Biol. 2: 71–78

Rahme LG, Ausubel FM, Cao H, Drenkard E, Goumnerov BC, Lau GW, Mahajan-Miklos S, Plotnikova J, Tan MW, Tsongalis J, Walendziewicz CL, Tompkins RG. 2000. Plants and animals share functionally common bacterial virulence factors. Proc. Natl. Acad. Sci. USA. 97: 8815-8821

Szabó G, Schulz F, Toenshoff ER, Volland JM, Finkel OM, Belkin S, Horn M. 2017. Convergent patterns in the evolution of mealybug symbioses involving different intrabacterial symbionts. ISME J. 11: 715–726

Thomashow LS, Weller DM. 1988. Role of a phenazine antibiotic from *Pseudomonas fluorescens* in biological control of *Gaeumannomyces graminis* var. *tritici*. J. Bacteriol. 170: 3499–3508

Turner JM, Messenger AJ. 1986. Occurrence, biochemistry and physiology of phenazine pigment production. Adv. Microbial Physiol. 27: 211–275

Vilaplana L, Marco MP. 2020. Phenazines as potential biomarkers of *Pseudomonas aeruginosa* infections: synthesis regulation, pathogenesis and analytical methods for their detection. Anal. Bioanal. Chem. 412: 5897–5912

Waack S, Keller O, Asper R, Brodag T, Damm C, Fricke WF, Surovcik K, Meinicke P, Merkl R. 2006. Score-based prediction of genomic islands in prokaryotic genomes using hidden Markov models. BMC Bioinformatics 7: 142

Wang Y, Wilks JC, Danhorn T, Ramos I, Croal L, Newman DK. 2011. Phenazine-1-carboxylic acid promotes bacterial biofilm development via ferrous iron acquisition. J. Bacteriol. 193: 3606–3617

Wattam AR, Abraham D, Dalay O, Disz TL, Driscoll T, Gabbard JL, Gillespie JJ, Gough R, Hix D, Kenyon R, Machi D, Mao C, Nordberg EK, Olson R, Overbeek R, Pusch GD, Shukla M, Schulman J, Stevens RL, Sullivan DE, Vonstein V, Warren A, Will R, Wilson MJ, Yoo HS, Zhang C, Zhang Y, Sobral BW. 2014. PATRIC, the bacterial bioinformatics database and analysis resource. Nucleic Acids Res. 42: D581–D591

Wick RR, Judd LM, Gorrie CL, Holt KE. 2017. Unicycler: resolving bacterial genome assemblies from short and long sequencing reads. PLoS Comput. Biol. 13: e1005595

Wilson R, Sykes DA, Watson D, Rutman A, Taylor GW, Cole PJ. 1988. Measurement of *Pseudomonas aeruginosa* phenazine pigments in sputum and assessment of their contribution to sputum sol toxicity for respiratory epithelium. Infect. Immun. 56: 2515–2517

Yu S, Vit A, Devenish S, Mahanty HK, Itzen A, Goody RS, Blankenfeldt W. 2011. Atomic resolution structure of EhpR: phenazine resistance in *Enterobacter agglomerans* Eh1087 follows principles of bleomycin/mitomycin C resistance in other bacteria. BMC Struct Biol. 11: 33